How do the novel substituted 3H-indole probe molecules reside in the AOT-based water-in-oil microemulsion? An investigation by absorption and fluorescence spectroscopy

Yilong Chen, Tongkuan Xu, Xinghai Shen*, Hongcheng Gao

College of Chemistry and Molecular Engineering, Peking University, Beijing 100871, PR China

Abstract

A surface-active substituted 3H-indole quaternary ammonium molecule, [2-(*p*-cetylaminophenyl)-3,3-dimethyl-5-ethoxycarbonyl-3H-indole] methyl dihexadecyl-ammonium iodide (**3**), was designed and synthesized in hexamethyl phosphoramide (HMPA). The product was purified and characterized by IR, ^{1}H NMR, MS and elemental analysis. Using **3** and its homologue [2-(*p*-dodecylaminophenyl)-3,3-dimethyl-5-ethoxycarbonyl-3H-indole] methyldihexadecyl ammonium iodide (**2**), we have measured the protonic association constant, the fluorescence anisotropy for the two molecules in the AOT-based water-in-oil (w/o) microemulsion, as well as the dielectric constant of the microemulsion interface sensed by **2** and **3**. The results provide further evidences supporting our previous viewpoint about the locations of different groups of this kind of substituted 3H-indoles in the microemulsion.
© 2004 Elsevier B.V. All rights reserved.

*Keywords:* Substituted 3H-indole; Fluorescence; w/o microemulsion; Hydrophobic interaction

1. Introduction

The investigation of the dynamics of the solubilization of probe molecules by reversed micelles or water-in-oil (w/o) microemulsions might contribute to the general understanding of transport processes through more complex membrane structure [1]. In these microheterogeneous membrane-mimetic systems, a probe molecule could be located in a variety of microenvironments, namely, the continuous organic phase, the water pool or the interface. Knowledge of the locations of molecular probes in w/o microemulsions could give information about their possible residing sites in the biological systems [2], and is thus of scientific importance. On the other hand, although fluorescent probe molecules are often used to study the physicochemical properties of microheterogeneous media, e.g., micropolarity and microviscosity [3–9], the reported values of these properties for similar systems

are not identical, partly resulting from the fact that the locations of different probes in such systems may be different. Therefore, it is important to obtain the information on the location of a fluorescent probe when it is used in sensing a certain microhetergeneous medium. Also, the knowledge of the microstructure of the microemulsion may contribute to explore the molecular template of polymer [10], the formation mechanism of nanoparticels [11–13] and supramolecular aggregates [14] in microemulsion.

In our previous work [8], we have explored the locations of different groups of a cationic surface-active 3H-indole probe molecule (molecule **1**, see Scheme 1) in the AOT-based w/o microemulsion. On the basis of the measured physicochemical properties of **1**, and also considering the hydrophobic interaction of the two aliphatic chains and the hexyl group with the interface of the microemulsion, the strong electrostatic interaction, as well as the location of the indolic nitrogen, we have suggested a relatively clear picture concerning the locations of different groups of **1** in the AOT-based microemulsion (Fig. 5 in reference

* Corresponding author. Tel.: +86 10 62753443; fax: +86 10 62759191.
E-mail address: xshen@pku.edu.cn (X. Shen).
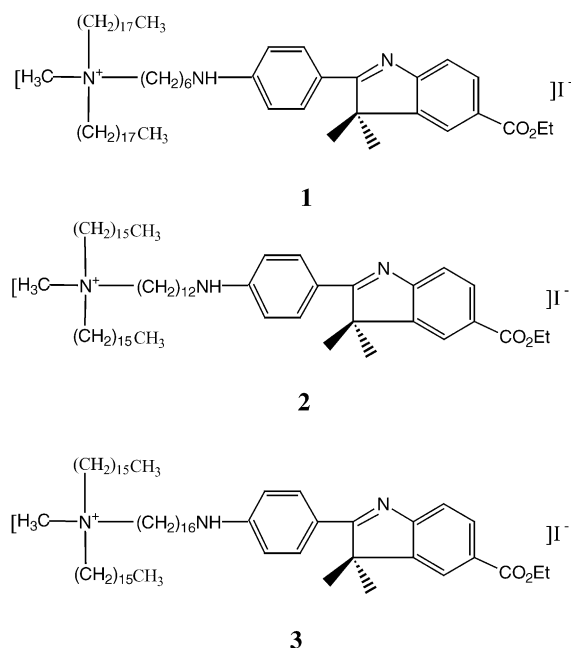
Scheme 1. Molecular structures of **1**–**3**.

8). One possible picture is that the aliphatic chains and the hexyl group together with the part from the amino nitrogen to the indolic nitrogen penetrate the interface, while the part from the indolic nitrogen to the right side resides in the water pool. The second possible picture is that the aromatic chain of **1** lies flat in the inner interface of the microemulsion [8].

To further confirm the above picture, we have synthesized molecules **2** and **3**. Besides the slight difference in the aliphatic chains, the group $-(CH_2)_6-$ in **1** was altered to $-(CH_2)_{12}-$ and $-(CH_2)_{16}-$, respectively. It is speculated that the different penetration extent of $-(CH_2)_{12}-$ and $-(CH_2)_{16}-$ groups into the microemulsion interface will lead to the different penetration extent of the aromatic chains for **2** and **3** [15]. Consequently, both the amino nitrogen and the indolic nitrogen protect from water interaction to a different extent.

This will bring about different behaviors in some physico-chemical properties of **2** and **3**.

Recently, we reported the formation of the 1:3 (guest:host) rotaxane-like inclusion complex between substituted 3H-indoles and β-cyclodextrin (β-CD) [16,17]. We have also investigated the interaction of substituted 3H-indoles with bovine serum albumin (BSA) and human serum albumin (HSA). Some preliminary results concerning the analytical application and the energy transfer phenomenon in the systems have been obtained [18]. It is believed that the present work can help understanding the hydrophobic interaction mechanism of supramolecular assemblies and especially the reaction patterns between the fluorescent probe and proteins.

2. Experimental section

2.1. Materials

2.1.1. Synthesis and characterization of **3**

The synthesis and purification of compound **8** (Scheme 2) have been carried out according to the methods of Skrabal et al. [19] and Popowycz [20]. Compound **5** was synthesized according to [21], and it reacted with compound **6** to afford compound **7** in CH_3CN under reflux for 18 h. Compound **3** was obtained from the reaction between compounds **7** and **8** in HMPA at 80 °C for 24 h. All the syntheses were performed under nitrogen atmosphere. Compounds **7** and **3** were purified by column chromatography with mixed solvents (dichloromethane:methanol = 70:1) and by recrystallization in acetone. The products were purified and characterized by IR, ^{1}H NMR, MS and elemental analysis.

Compound **7** (75.9%), IR (KBr) ν (cm^{-1}): 3442, 2917, 2850, 1636, 1470, 1163, 718. ^{1}H NMR (300 MHz, CDCl$_3$, TMS) δ/ppm: 0.88 (t3H, $-CH_3$, J = 6.6 Hz), 1.26–1.82 (m, 84H, $-CH_2-$), 3.17–3.41 (m, 11H, N–CH$_3$, N–CH$_2-$, I–CH$_2-$). MS m/z: 830 (M$^+$ − 127 + 1).

Compound **3** (20%), IR (KBr) ν (cm^{-1}): 3428, 2920, 2851, 1713, 1604, 1467, 1313, 1232, 1107, 779. ^{1}H NMR
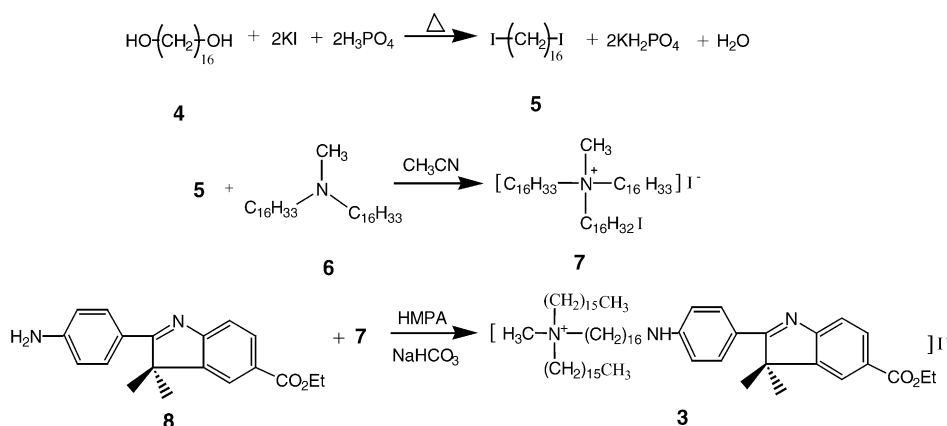
Scheme 2. Synthesis route of molecule **3**.

(300 MHz, CDCl$_3$, TMS) δ/ppm: 0.88 (t, 6H, –CH$_3$, J = 7.04 Hz), 1.25–1.68 (m, 93H, –CH$_2$–, –CH$_3$), 3.31–3.45 (m, 11H, N–CH$_2$–, N–CH$_3$), 4.35–4.40 (m, 3H, –CH$_2$–O, –NH–), 6.60 (d, 1H, Ph–H), 7.60 (d, 1H, Ph–H), 7.80 (m, 1H, Ph–H), 7.98–8.07 (m, 3H, Ph–H), 8.36 (s, 1H, Ph–H). MS m/z: 1010 (M$^+$ − 127 + 1). Elemental analysis for C$_{68}$H$_{120}$N$_3$O$_2$I·H$_2$O, calculated: (C 70.65%, H 10.56%, N 3.64%); found: (C 69.96%, H 10.54%, N 3.25%).

The synthesis and purification of **2** have been described elsewhere [22]. AOT (Sigma, 99% purity) was purified by the methods of Seoud and Da Silva [23]. *n*-Heptane was re-distilled over metallic sodium, and *n*-hexanol, *n*-pentanol, *n*-butanol, *n*-propanol, ethanol and methanol were redistilled after being dried with anhydrous sodium sulfate for about 24 h. Sodium hydroxide, sodium carbonate, sodium bicarbonate, potassium acid phthalate, hydrochloric acid were analytical grade reagents and used without further purification. Tridistilled water was used throughout the experiments.

2.2. Instruments

aAbsorption spectra were recorded on an UV-3100 (Shimadzu) spectrophotometer using 1-cm path quartz cells. The slit width was 5 nm. Fluorescence spectra were measured on a FL-4500 (Hitachi) spectrofluorimeter. The excitation wavelengths were close to the absorption wavelengths of each sample contained in 1-cm path quartz cells. Anisotropy values were measured on a FL920 Combined Fluorescence Lifetime and Steady State (Britain, Edinburgh) spectrofluorimeter. Both the excitation and emission band passes were 5 nm for **2** and **3**. The excitation wavelengths were 380 and 385 nm for **2** and **3**, respectively, in all the fluorescence experiments.

2.3. Methods

The preparation of the w/o microemulsions containing probe molecules and their pH adjustments were performed according to the same methods as described in [8]. The concentration of **2** and **3** for the absorption studies was 6 × 10^{-6} M, while that for both steady-state fluorescence and anisotropy measurements was 1 × 10^{-6} M. Stock solutions of **2** and **3** in methanol and of AOT (0.5 M) in *n*-heptane were prepared for analyses. All measurements were done at room temperature.

3. Results and discussion

3.1. Absorption spectra

Recently, pH effect studies of substituted 3H-indoles in water, micelles, reversed micelles and β-CD have shown that the first preferred site of protonation is the indolic nitrogen atom [8]. According to the literature [8,16,17,24,27], water and hydrogen ion can act as a hydrogen bond donor to the electron lone pair of the nitrogen atom of the indolic nitrogen,
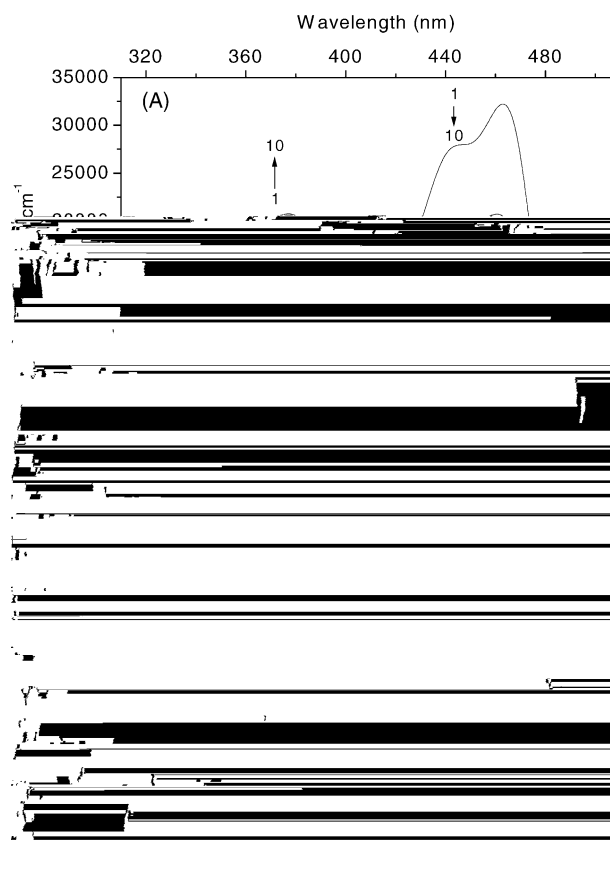

Fig. 1. Absorption spectra of **2** (A) and **3** (B) in the AOT-based w/o microemulsion (R = 15) at various pH values: 1.0 (1); 2.0 (2); 3.0 (3); 4.0 (4); 5.0 (5); 6.1 (6); 7.1 (7); 8.0 (8); 9.0 (9); 10.0 (10).

which would cause reduced conjugation of phenyl ring with the indolic moiety, leading to a red-shift in the absorption band. For **1**, the different behaviors of pH effect in water, micelles and reversed micelles composed of anionic, cationic or nonionic surfactants have been observed [8,24].

To substantiate the previous viewpoints concerning the location of the fluorophores in the w/o microemulsion and to prove that the aromatic chains of the fluorophores penetrate to the interface to a different extent, we have carried out the pH effect study of **2** and **3**. Fig. 1 shows the absorption spectra of **2** and **3** in the w/o microemulsion at R = 15 (R = [H$_2$O]/[AOT]). On decreasing the pH value, a largely red-shifted, highly intense and structured band is formed. Isosbestic points λ_{iso} = 412.4 and 407.0 nm of **2** and **3** (see Fig. 1 and Table 1) are also observed, which suggests the presence of two species only in each system. The phenomena are similar to that of **1** in the w/o microemulsion [8]. These results could be interpreted in terms of the protonation of the indolic nitrogen to form mono-cation [8,24]. And Fig. 2 shows that the absorbance at 375 nm (Fig. 2(A)) increases with increasing pH value; however, the absorbance obtained at 460 nm exhibits an opposite trend (Fig. 2(B)). It seems that the absorbance of **3** is relatively insensitive to the change of acidity as compared with that of **2**.

Table 1
The protonic association constants and spectral characteristics of **2** and **3** in the AOT-based w/o microemulsion

	K (M^{-1})			λ_{iso} (nm)	(M^{-1} cm^{-1})	
	$\lambda = 375$ nm	$\lambda = 460$ nm	Average		$\lambda = 375$ nm	$\lambda = 460$ nm
Molecule **2**	16.4 ± 0.8	15.2 ± 0.8	15.8	412.4	2.1×10^4	3.2×10^4
Molecule **3**	1.89 ± 0.8	2.18 ± 0.8	2.04	407.0	1.9×10^4	2.7×10^4

In order to evaluate quantitatively the different protonation between **2** and **3**, we considered the following equilibrium

$$L + H^+ \rightleftharpoons LH^+ \tag{1}$$

where L, LH$^+$ denote the fluorescent molecule and its protonated form, while K is the protonic association constant. The absorption peak at 375 nm belongs to L, nonprotonated 3H-indoles, while the peak at 460 nm can be attributed to LH$^+$, protonated 3H-indoles [8,24]. A chemical balance between L and LH$^+$ exists. Reliable K values could be obtained by the use of linear fit according to the following equation [25,26]

$$\text{Log}\left[\frac{(\quad - \quad_{LH^+})}{(\quad_L - \quad)}\right] = pH + p \tag{2}$$

where A, $\quad_{LH^+}$ and A_L represent the absorbance, and those at high acidity where LH$^+$ dominates in the sample as well as at low acidity where L dominates in the sample. These values were measured at a same wavelength. Fig. 3 shows the excellent linear relationship with correlation coefficients (r) larger than 0.99. The K values obtained at 375 nm (Fig. 3(A)) and 460 nm (Fig. 3(B)) are identical within the experiment

error (Table 1). Also, one could notice that the protonic association constant of **2** is obviously larger than that of **3** in the w/o microemulsion.

The protonic association constants reflect the association degree of the hydrogen as a donor to the acceptor. As mentioned above, the first preferred site of protonation is the indolic nitrogen atom. Thus, comparing the value of the two kinds of the 3H-indole quaternary ammonium molecules in AOT, we can conclude that the hydrogen ion is easier to approach the indolic nitrogen of molecule **2** than that of **3**. This leads us to conclude that the aromatic chain of **3** penetrates into the interface more deeply than that of **2**.

3.2. Fluorescence spectra

The fluorescence spectra of **3** at various pH values are illustrated in Fig. 4(A). It can be seen from Fig. 4(B) that the fluorescence intensity is increased rapidly with increasing pH, and then reaches plateau at pH = 5.6. The similar phenomenon was observed for **2** (the fluorescence spectra not
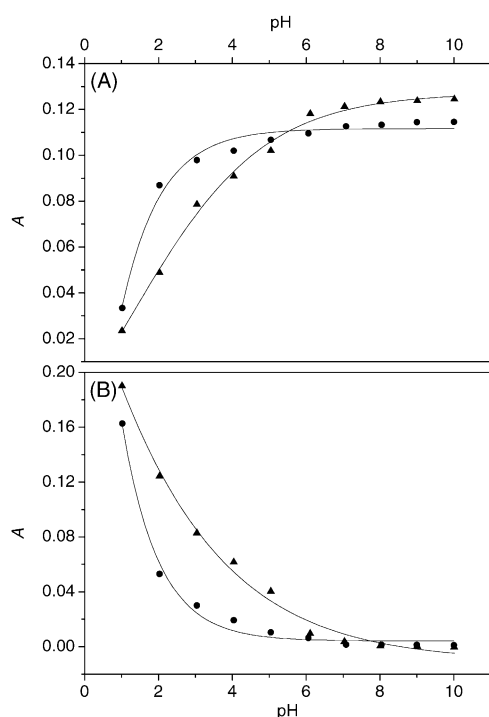

Fig. 2. Absorbance (A) obtained at 375 nm (A) and 460 nm (B) versus pH for molecules **2** (▲) and **3** (●) in the AOT-based w/o microemulsion ($R = 15$).
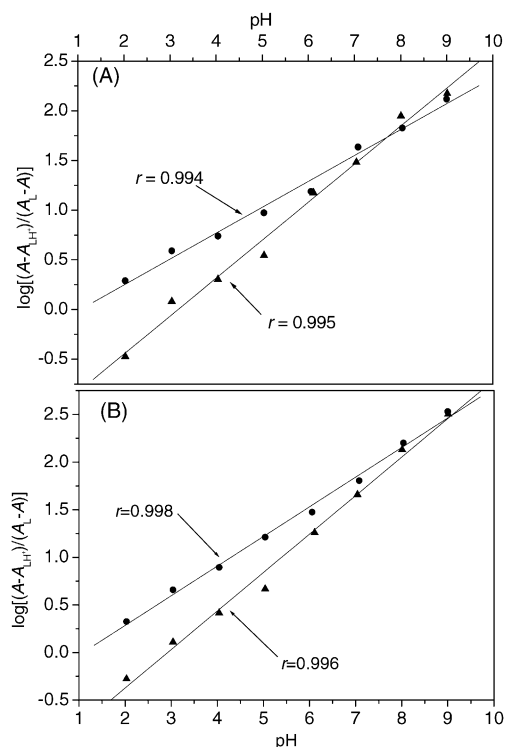

Fig. 3. Log[($\quad - \quad_{LH^+}$) ($\quad_L - \quad$)] versus pH for molecules **2** (▲) and **3** (●) in the AOT-based w/o microemulsion ($R = 15$) at 375 nm (A) and 460 nm (B).
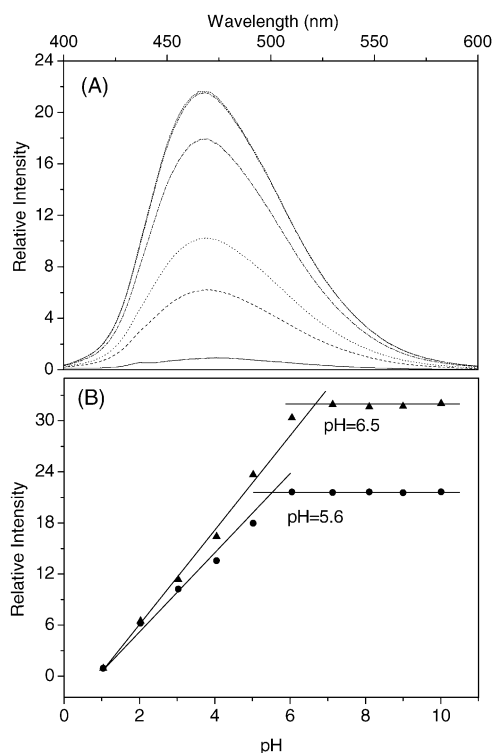
Fig. 4. (A) The fluorescence spectra of **3** at different pH: 1.04 (solid), 2.03 (dash), 3.03 (dot), 5.02 (dash dot), 6.05 (dash dot dot), 10.01 (short dot). (B) Variation of fluorescence intensity of molecules **2** (▲) and **3** (●) with pH in the AOT-based w/o microemulsion ($R = 15$).

shown). Fig. 4(B) also shows that the fluorescence intensity of **2** reaches plateau at pH = 6.5. These molecules belong to the unique 3H-indolic molecule, which is not rigid, and that the phenyl ring can liberate within the kT energy barrier. This torsional movement is responsible for the geometric changes taking place in the ground and excited states and provides an importance deactivation pathway for the S_1 state. According to the INDO/S semi-empirical calculations, this main nonradiative decay pathway has been ascribed to the formation of a nonemissive twisted intramolecular change transfer (TICT) state originating in the amino group [5,27]. This is the reason why the fluorescence intensity of **2** and **3** is small at lower pH values. It is noticed that the fluorescence intensity of **3** reaches plateau at a smaller pH value as compared with **2**. Again, this result indicates that the hydrogen ion approaches more difficultly to the indolic nitrogen of **3** than that of **2**.

3.3. The anisotropy and micropolarity measurements

The fluorescence intensity of a molecular probe is influenced by viscosity and polarity, and it is larger in the lower polarity and/or higher viscosity solubilization sites [4,6,7,9,24,27], since the formation of TICT state involves the rotation of the amino groups. As R increases, the hydrodynamic radius of the water pool of AOT-based microemulsion exhibits linear relationship with R, i.e., r_w (nm) = $0.175R + 1.5$ [28–31].

3.3.1. The anisotropy measurement

The investigation performed by Hasegawa et al. [6] showed that in the AOT-based microemulsion, the microviscosity of the water pool at the vicinity of the AOT anionic head group falls abruptly up to $R = 10$ and then gradually decreases until the upper limit of the water solubilization using the viscosity-sensitive auramine O (AuO), which locates in the water pool. And using the cationic dye phenosafranin (PSF), Chaudhuri and co-workers found that the fluorescence polarisation anisotropy is increased by increasing R up to 10, indicating an increase in the rigidity of the dye environment [7]. Moreover, it was found that the viscosity of the AOT reversed micelles is appreciably higher than that of the bulk water [6,7,27]. Molecules **2** and **3** belong to the unique class of fluorophore in which the deactivation of the excited singlet state is principally governed by a nonradiative internal conversion ascribed to intramolecular torsional relaxation. Any restrictions imposed on the excited-state torsion of the fluorophore, e.g., the increase in the viscosity of the solvating medium, are essentially reflected in the fluorophore's nonradiative decay rate [27]. Fig. 5(A) shows the variation of anisotropy (r) of **2** and **3** with R in the w/o microemulsions. It can be seen that the anisotropy (r) increases with increasing water content up to $R = 10$, and then reaches a constant. Also, one can notice that the anisotropy (r) of **3** is larger than that of **2**. The difference between the anisotropy (r) of molecules **2** and **3** indicates that the penetration extent of **3** into the interface is larger than that of **2**.
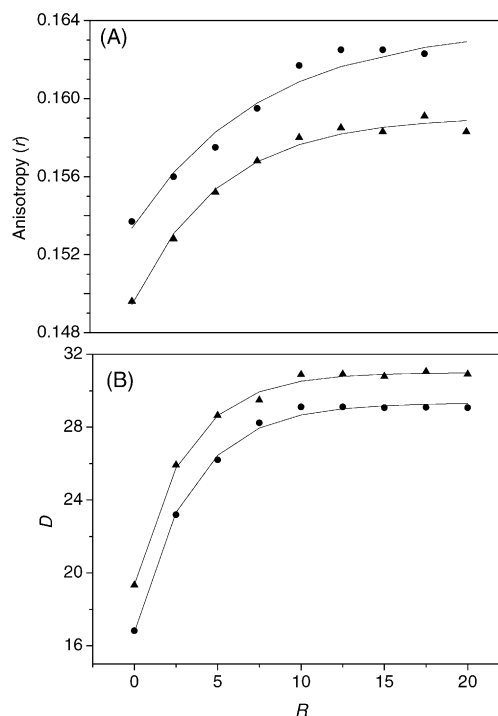

Fig. 5. Variation of anisotropy (A) and dielectric constant (B) of **2** (▲) and **3** (●) with R in the AOT-based w/o microemulsion. The experimental data were fitted using Eqs. (5) and (6).

3.3.2. The micropolarity measurement

In order to estimate the polarity value and the nature of the binding sites of **2** and **3** in the above-mentioned organized assemblies according to the method described in the literature [3,5,8,24,27], the following correlation, between the Stokes shift (reciprocal centimeters) and dielectric constant (*D*) for **2** and **3** in alcohols of increasing chain length (methanol to hexanol) and water, has been obtained

$$\text{For 2}: \quad (\nu_{ex} - \nu_{em})(\text{cm}^{-1}) = 33\ 17 \quad + 4321 \tag{3}$$

$$\text{For 3}: \quad (\nu_{ex} - \nu_{em})(\text{cm}^{-1}) = 33\ 55 \quad + 4348 \tag{4}$$

From the two equations, the micropolarity values for AOT-based microemulsions have been estimated. The results are shown in Fig. 5(B). It can be seen from the plot that the *D* values reported by **2** and **3** are 19.3 and 16.8 at *R* = 0. With the further addition of water, the *D* value increases rapidly and then reaches a plateau at *R* = 10, which is in good agreement with the result in the literature [3,5]. In Fig. 5(B), it shows that the micropolarity of **3** is smaller than that of **2** at same *R* values. Again, this means that the indolic and phenyl rings of **3** reside more deeply into the interface as compared with **2** because of the stronger hydrophobic interaction of the cetyl group than that of the dodecyl group with the interface.

Furthermore, the experimental data (Fig. 5) can be fitted using the following equations

$$= {}_1(1 - \exp(- {}_1\ )) + {}_1 \tag{5}$$

$$= {}_2(1 - \exp(- {}_2\ )) + {}_2 \tag{6}$$

For molecule **2**,

[24] J. Li, X. Shen, H. Gao, Spectrosc. Spect. Anal. 21 (2001) 508.

[25] A. Albert, E.P. Serjeant, Ionization Constants of Acids and Bases, Mathuen & Co, New York, 1962.

[26] G.W. Ewing, Instrumental Methods of Analysis, McGraw-Hill Book Co, New York, 1985.

[27] M. Belletête, R.S. Sarpal, G. Durocher, Can. J. Chem. 72 (1994) 2239.

[28] J.D. Nicholson, J.H.R. Clarke, Surfactants in solution, in: K. Mittal, B. Lindman (Eds.), Proceedings of the International Symposium, vol. 3, Plenum Press, New York, 1984, p. 1663.

[29] P.D.I. Fletcher, A.M. Howe, B.H. Robinson, J. Chem. Soc., Faraday Trans. 1 83 (1987) 985.

[30] A. Maitra, J. Phys. Chem. 88 (1984) 5122.

[31] X. Shen, H. Gao, X. Wang, Phys. Chem. Chem. Phys. 1 (1999) 463.